Chalcogenide Letters Vol. 16, No. 11, November 2019, p. 557 - 563

CONCENTRATION EFFECTS ON ELECTRONIC AND SPECTROSCOPIC PROPERTIES OF ZnCdS WURTZOIDS: A DENSITY FUNCTIONAL THEORY STUDY

M. T. HUSSEIN[a,*], T. A. FAYAD[a], M. A. ABDULSATTAR[b]
[a]*Department of Physics, College of Science, University of Baghdad, Baghdad, Iraq*
[b]*Ministry of Science and Technology, Baghdad, Iraq*

In the present work, ternary compound $Zn_{1-x}Cd_xS$ wurtzoid is investigated using density functional theory with variable Zn and Cd contents. Electronic and spectroscopic features of $Zn_{1-x}Cd_xS$ wurtzoid are investigated including energy gap, the density of states, bond lengths, spectroscopic properties including IR and Raman spectra. Longitudinal optical mode frequency of IR and Raman is compared with experimental results. Theoretical results are in good agreement with experimental and previous results. It is found that energy gap decreases when the concentration of Cd increases, and the longitudinal optical mode has a red shift with increasing concentration.

(Received July 27, 2019; Accepted November 22, 2019)

Keywords: ZnCdS, Wurtzite, Raman

1. Introduction

ZnCdS is one of the essential Chalcogenide semiconductors belonging to group II-VI in the periodic table that has a wide energy direct optical band gap. The gap of the band is a very significant parameter to determine the optical and electronic characteristics of semiconductors. Because of the discrete band gaps, binary semiconducting nanocrystals were restricted in the applications. The ternary semiconductor materials (like ZnCdS) however have adjustable band energy [1, 2]. Latterly, the investigation of ternary nanocrystals of ZnCdS has attracted several academics and experts. It provides the properties of direct band gap, coefficients of high absorption in the regions of blue and UV, and performance between ZnS and CdS. For instance, composition-tunable band gap width and size-tunable from (2.4 to 3.7) eV [1, 2] is obtained. The structural characteristics of semiconducting materials alloy vary from the ZnS binary and CdS nanocrystal binary compound [2, 3]. In addition to that, the CdS and ZnS of zinc blend lattice constants are at room temperature around 5.406 and 5.835 Å for the zincblende structure. The small lattice mismatch enables Zn to be taken into the CdS lattice to form ternary alloyed quantum dots [4, 5]. The optical band gap (Eg) for the ternary film of ZnCdS was discussed by implementing spectra reflection in the wavelength range (325-600 nm) [6, 7]. The ternary ZnCdS is steadier under irradiation than ZnS and has a wide variety of visible light absorption [8].

ZnCdS has characteristics between those ZnS and CdS due to ZnS offers a broader band gap and a greater optical transmittance comparison with CdS that is considered vital in the applications of solar cells [9–11]. It is appropriate for computer and other devices applications due to it is well-recognized optical parameters like reflectance, refractive index, optical transmittance, and optical band gap [10]. The quantum confinment impact on the optical characteristics of nanocrystal materials are considerably different from the respective bulk and based on the size of the crystallite. [12].

In this study, geometrical, electronic and spectroscopic characteristics of the nanostructures of ZnCdS as wurtzoids is investigated using Ab initio methods dependent on Density Functional Theory (DFT).

* Corresponding author: mudarahmed3@yahoo.com

2. Theory

In this work, we employed theoretical ab-intio methods to simulate the features and nanostructures of $Zn_{1-x}Cd_xS$ wurtzoid molecule; the present approach uses all electrons density functional theory B3LYP (Becke, three-parameters, Lee-Yang-Parr) with 3-21G basis sets. Using B3LYP\3-21 G means the utilizing of 0.965 scale factors to correct frequencies of vibrational [13]. All calculations are made utilizing the software of Gaussian 09 [14]. In this study, the molecular-nanoscale limited of $Zn_{1-x}Cd_xS$ as functions of concentration is investigated.

The researchers were working to form the wurtzoids molecules at nanoscale limited that can be in wurtzite phase structure (a=b≠c) of material [15] and using simulation by programs Gaussian 09. The considered structures of wurtzoids involve the Zn_7S_7, Cd_7S_7, and $Zn_2Cd_5S_7$ as shown in the Fig. 1 at nanoscale size.

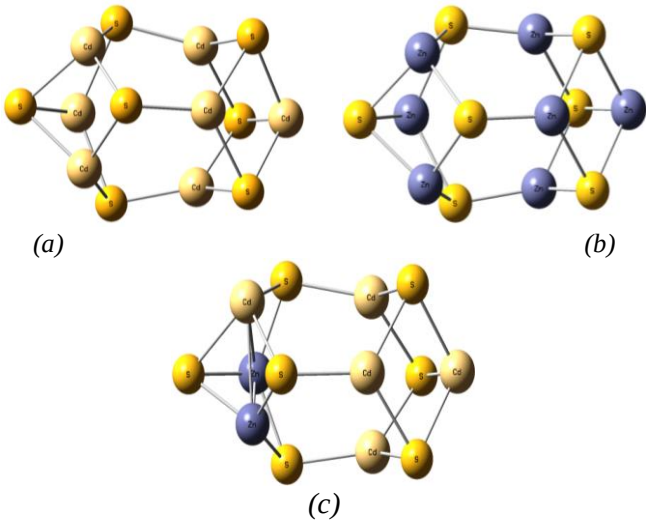

Fig. 1. Represent the geometry of A) Cd_7S_7 B) Zn_7S_7 C) $Zn_2Cd_5S_7$ wurtzoids nanotubes structure after optimization.

3. Experimental results and discussions

3.1 Electronic characteristics

The current work an investigation for the variation of the concentration (x) of $Zn_{1-x}Cd_xS$ Wurtzoids as a function of energy gap where it was observed that the reduction in the magnitudes of energy gaps had been achieved if Cd concentration increases as demonstrated in figure (2). Eg for all content of Cd was higher than Eg of bulk $Zn_{1-x}Cd_xS$. The levels of energy are restricted to possible small-scale wells. Peter and Lee reported the same conduct [16]. They draw the energy band gap vs. content of Cd for bulk and experimental $Zn_{1-x}Cd_xS$. This conduct is to reduce the height of the barrier. Band gap rise is occurring when the crystal becomes narrower, so the energy gap appears higher than the bulk [17, 18]. The variation in Eg magnitudes is in line with the experimental outcomes in Ref. [19]. Therefore, it was noticeable that as the energy gaps at nanoscale increasing due to quantization confinement. Therefore, the gaps of energy values for bulk are found tuning between (3.7-2.4) eV [17, 18], and experimental thin film between (4-2.55) eV [19]. And theoretical values of binary Zn_7S_7, Cd_7S_7, and ternary $Zn_2Cd_5S_7$ is (3.24, 3.03, 3.2) eV respectively.

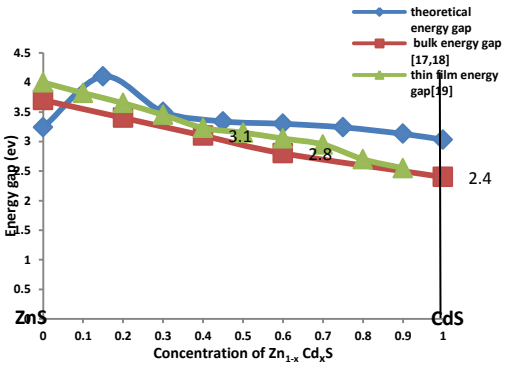

Fig. 2. Energy gaps of $Zn_{1-x}Cd_xS$ as a function of the concentration of atoms Zn, Cd and S and compare with the experimental bulk [17, 18], thin film [19] of ZnS and CdS wurtzoids.

3.2. Density of states

In Fig. (3 A, B, C) show the Densities of state of ternary $Zn_2Cd_5S_7$ wurtzoid and binary (Cd7S7, Zn7S7) wurtzoids as a function of the energy level of them after optimization geometric the density of states is increase when a decrease of concentration. It found that the energy band gap between high and low occupied molecular orbital (V.B and C.B) respectively of ternary wurtzoids is variation and tunable about the experimental value of Cd_7S_7 and Zn_7S_7 in range (3. 25-2.99) eV.

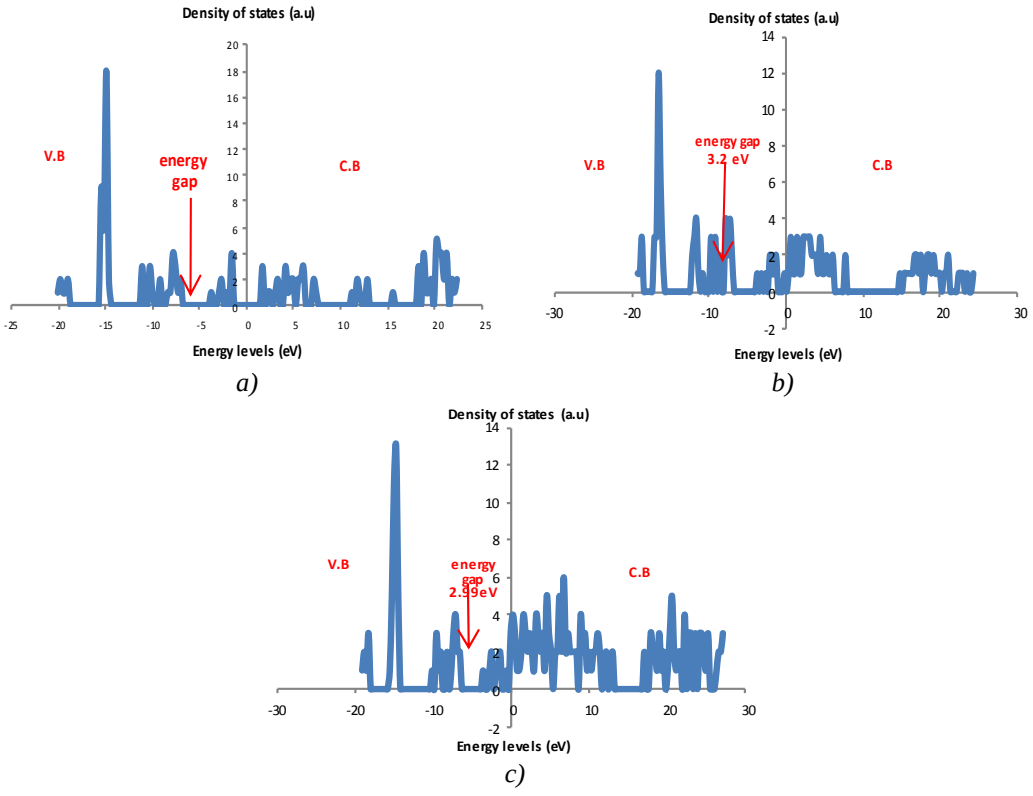

Fig. 3. (A) Density of state of Zn_7S_7 wurtzoids as a function of energy levels (B) Density of state(DOS) of $Zn_2Cd_5S_7$ wurtzoid as a function of energy levels (C) Density of state of Cd_7S_7 wurtzoid as a function of energy levels.

3.3. Density of bonds

Fig. 4 illustrates that distribution of density of bonds length of $Zn_2Cd_5S_7$ wurtzoids and compare with experimental values of bonds. There are two types of bonds exist, i.e. Zn-S and Cd-S [20, 21]. The strong bond length is Zn-S bonds followed by Cd-S bonds. These bonds values are

in agreement with experimental values. The widest distribution because the calculations are like surface calculation in which reconstruction deviates many bond from their ideal length.

The experimental values of the above bonds are (2.34 and 2.55) A respectively [20, 21] the reason belongs to type the bonds of sp2 as well-known be short and strong on inverse sp3 bonds.

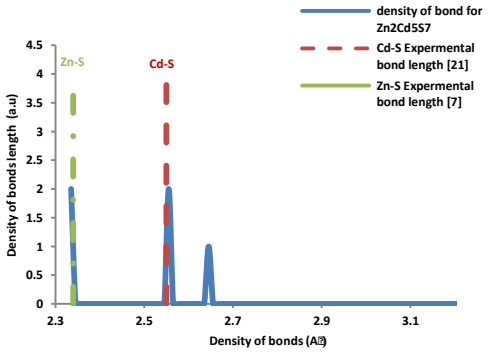

Fig. 4. The density of bonds of $Zn_2Cd_5S_7$ wurtzoid (Comparison with bulk experimental wurtzite value [7, 21]).

4. Spectroscopic properties

4.1. Longitudinal optical

Fig. 5 illustrates the longitudinal optical (LO) vibrational mode of $Zn_2Cd_5S_7$ wurtzoid as a Cd concentration (x) function. The nanoscale impact is to decrease the frequency of the LO mode value [22]. Additionally, due to the dangling bonds from the surface, the bare case has greater frequencies. The impact of dangling bonds is to raise the steady force, as demonstrated in Figure 5. The LO is identical to experimental LO mode at the ZnS boundary. The LO modes will converge with the experimental value of CdS when increasing the concentration.

The theoretical values of wurtzoids in Fig 5 are two modes 355 and 304.61 cm^{-1}. Comparison these values with experimental ZnS and CdS LO modes (351 and 305 cm-1 respectively [7, 23]) it can be shown that the current technique estimates are in good agreement with experiment.

The variation of ZnS, $Zn_2Cd_5S_7$, and CdS wurtzoids vibrational mass decrease, respectively as a function of frequency can be seen in Figure 6. The bare molecules have a broad decreased mass because their atoms are not connected to other atoms that substantially reduce the reduced mass value. Ultimately, heavy atoms or heavy collection of atoms vibrate first and have the lowest frequencies according to the equation. [24]:

$$\nu = \frac{1}{2\pi}\sqrt{\frac{k}{\mu}}$$

Whereas:

K: is the force constant,

μ: is the reduced mass.

The last mode, in this case, is the longitudinal optical mode (LO). Fig 7 demonstrates the variation of ZnS, $Zn_2Cd_5S_7$, and CdS wurtzoids vibrational force constant respectively as a frequency function. Therefore the similar results for both Fig 6 and Fig 7 are obtainable. In the two figures, it could be observed that the vibrations are Red shifted.

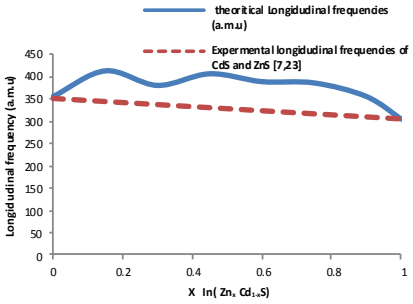

Fig. 5. Longitudinal optical (LO) Zn_{1-x} Cd_xS wurtzoids as a function of Cd concentration (x). The experimental bulk LO mode vibrational frequency of both CdS and ZnS [7, 23] as shown.

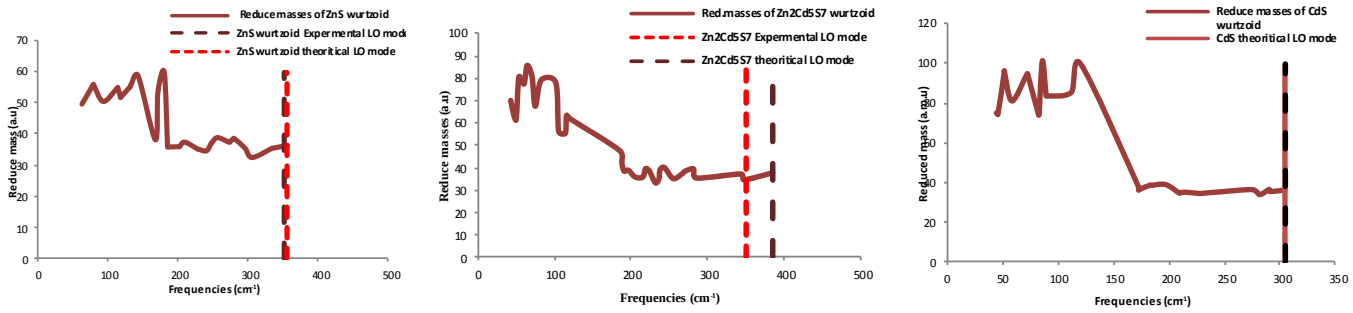

Fig. 6. The variation of ZnS, $Zn_2Cd_5S_7$, CdS wurtzoid vibrational reduced mass as a function of frequency. The experimental LO vibrational mode of both CdS and ZnS [7,23] as show.

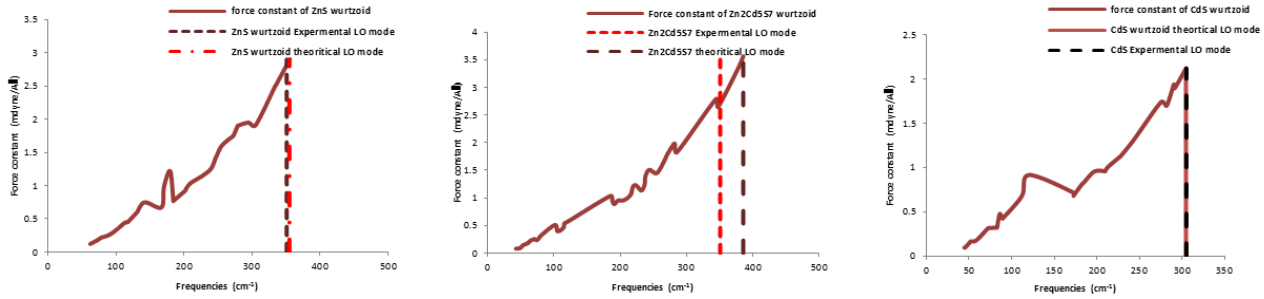

Fig. 7. The variation of ZnS, $Zn_2Cd_5S_7$, CdS wurtzoids vibrational force constant as a function of frequency .the experimental LO vibrational mode of both CdS and ZnS [7, 23] as shown.

4.2. IR and Raman spectra

Figs. 8 (A, B, C, D, E, and F) show IR and Raman spectra for ZnS, $Zn_2Cd_5S_7$, and CdS wurtzoids structure. Figure 8 (A) is observed in regions for (355.2) $cm^{-1,}$ and Raman spectra are very low intensity in these band. While figure (C) wurtzoid have various bands at two regions at (278.1) cm^{-1} and Raman spectra are observed at 359.1 cm^{-1} very low intensity in these bands and figure (E) wurtzoid have various bands at (305.5) cm^{-1} and Raman spectra observe at 303.8 cm^{-1} are very low intensity in these bands. While the experimental of LO frequencies for CdS and ZnS is (305,351) $cm^{-1,}$ respectively [23]. That means the theoretical value in agreement with experimental. the results in the present work are agreement with the result of ternary compound wurtzoids[24].

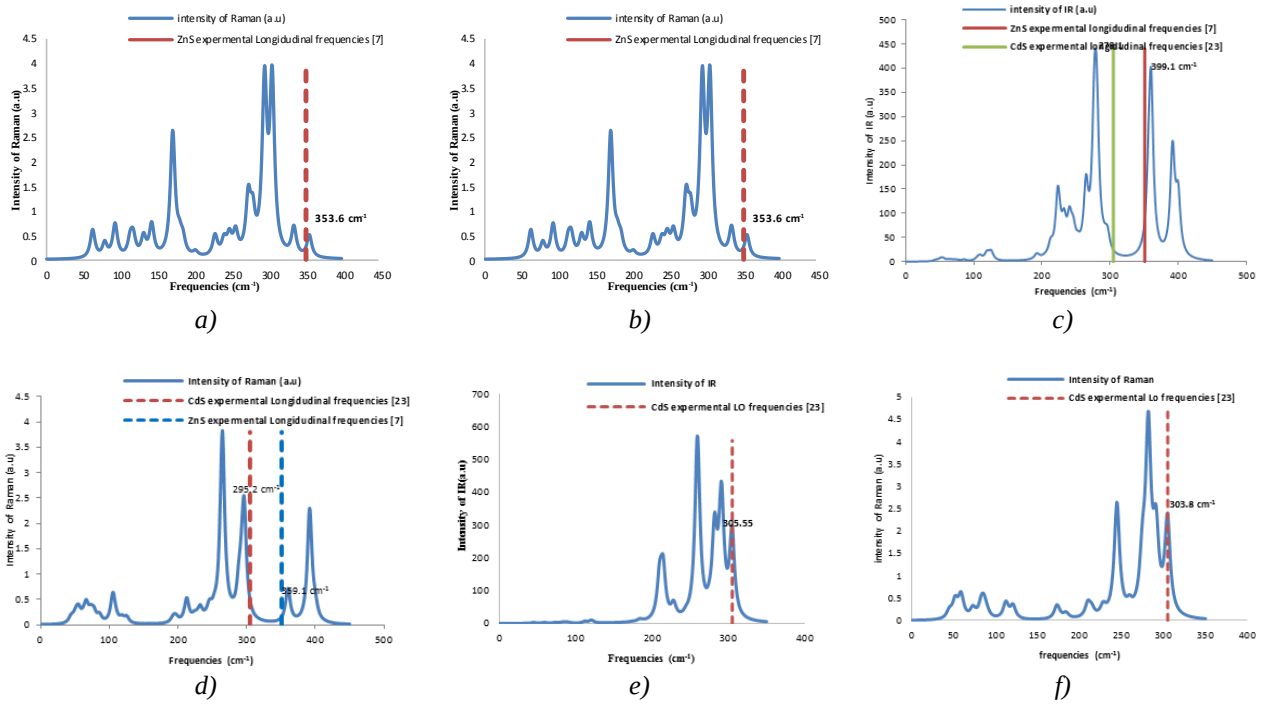

Fig. 10. IR and Raman spectrum for wurtzoids.
(a) IR of Zn_7S_7 Wurtzoid, (b) Raman of Zn_7S_7 Wurtzoid, (c) IR of $Zn_2Cd_5S_7$ Wurtzoid
(d) Raman of $Zn_2Cd_5S_7$ Wurtzoid. Compare with the CdS experimental LO vibrational mode (e) IR of Cd_7S_7 Wurtzoid,
(f) Raman of Cd_7S_7 Wurtzoid.

5. Conclusions

In the current work, we have shown that the utilizing of Nano-Wurtzoid crystals could provide an appropriate pattern of values for the vibrational and electronic characteristics of ZnCdS-Wurtzite materials. The two ZnCdS limits of composition, for example, ZnS and CdS, are reversed due to the presence of d orbitals in the heavier Cd atom and other structural and electronic variances between atoms of Zn and Cd. It found that the experimental gap of the energy value of binary bulk CdS and ZnS are nearer to the theoretical results of CdS and ZnS wurtzoids while the gap of the energy value of ternary ZnCdS Wurtzoidis decreased when increasing the concentration of Cd. The Longitudinal optical of $Zn_{1-x}Cd_xS$ wurtzoid has a red shift with increase concentration.

References

[1] M. Yang, Y. Wang, Y. Ren, E. Liu, J. Fan, X. Hu, Journal of Alloys and Compounds 2018.
[2] X.M. Liu, Y. Jiang, F. M. Fu, W. M. Guo, W. Y. Huang, L. J. Li, Facile, Mater. Sci. Semicond. Process, 16 (2013).
[3] M. T. Hussein, H. A. Fayadh, Chalcogenide Letters **13**(12), 537 (2016).
[4] J. Y. Ouyang, C. I. Ratcliffe, D. Kingston, B. Wilkinson, J. M. J. Kuijper, X. H. Wu, A. R. John, K. Yu, J. Phys. Chem. C, 112 (2008).
[5] M. T. Hussein, A. Ramizy, B. K. Ahmed, H. A .Fayadh, Journal of Non-Oxide Glasses **8**(2), 37 (2016).
[6] Mudar Ahmed Abdulsattar, Mohammed T. Hussein, Hadeel Ali Hameed, AIP Advances **4**, 127119 (2014).
[7] M. T. Hussain, H. A. Thjeel Chalcogenide letters **15**, 523 (2018).
[8] X. Q. Li, D. E. Yin, S. Z. Kang, J. Mu, J. Wang, G. D. Li, Colloids Surf. A **384**, 749 (2011).
[9] M. A. Mahdi, J. Basrah Res. (Sci.) **32**, 44 (2006).
[10] L. S. Ravangave, U. V. Biradar, Mater. Phys. Mech. **16**, 25 (2013).

[11] S. D. Chauvin, R. P. Sharma, J. Phys. Chem. Solids **66**, 1721 (2005).
[12] V. Singh, P. Chauhan, J. Phys. Chem. Solids **70**, 1074 (2009).
[13] NIST Computational Chemistry Comparison and Benchmark Database NIST Standard Reference Database Number 101 Release 18, October 2016, Editor: Russell D. Johnson III [Accessed: 29-Jan-2017].
[14] M. J. Frisch, G. W. Trucks, H. B. Schlegel, G. E. Suzerain, M. A. Robb, J. R. Cheeseman, J. A. Montgomery, Jr., T. Vreven, K. N. Kudin, J. C. Burant, J. M. ,Millam, S. S. Iyengar, J. Tomasi, V. Barone, B. Mennucci, M. Cossi, G. Scalmani, N. Rega, G. A. Petersson, H. Nakatsuji, M. Hada, M. Ehara, K. Toyota, R. Fukuda, J. Hasegawa, M. Ishida, T. Nakajima, Y. Honda, O. Kitao, H. Nakai, M. Klene X. Li, J. E. Knox, H. P. ,Hratchian, J. B. Cross, C. Adamo, J. Jaramillo, R. Gomperts, R. E. ,Stratmann, O. Yazyev, A. J. Austin, R. Cammi, C. Pomelli, J. W. ,Ochterski, P. Y. Ayala, K. Morokuma, G. A. Voth, P. Salvador, J. J. Dannenberg, V. G. Zakrzewski, S. Dapprich, A. D. Daniels, M. C. , Strain, O. Farkas, D. K. Malick, A. D. Rabuck, K. Raghavachari, J. B. Foresman, J. V. Ortiz, Q. Cui, A. G. Baboul, S. Clifford, J. Cioslowski, B. B. Stefanov, G. Liu, A. Liashenko, P. Piskorz, I. Komaromi, R. L. Martin, D. J. Fox, T. Keith, M. A. Al-Laham, C. Y. Peng, A. Nanayakkara, M. Challacombe, P. M. W. Gill, B. Johnson, W. Chen, M. W. Wong, C. Gonzalez, J. A. Pople, Gaussian, Inc., Pittsburgh PA, (2003).
[15] V. P. Kumar, A. Y. Sharma, D. K. Sharma, D. K. Dwivedi, Effect of sintering aid (CdCl2) on the optical and structural properties of CdZnS screen-printed film, Opt. Int. J. Light Electron. Optics **125**, 1209 (2014).
[16] A. JohnPeter, C. Lee, Chin. Phys. B **21**(8), 087302 (2012).
[17] T. P. Sharma, D. Patidar, N. S. Saxena, K. Sharma, Indian J. Pure Appl. Phys. **44**, 125 (2006).
[18] M. A. Mahdi, S. K. Al-Ani, Int. J. Nanoelectron. Mater. **5**, 11 (2012).
[19] T. Koga, J. Nitta, H. Takayanagi, S. Datta, Phys. Rev. Lett. **88**, 126601 (2002).
[20] Mohammed T. Hussein, Hanan A. Thjeel, IOP Conf. Series: Journal of Physics: Conf. Series, 1178 (2019).
[21] Poslet M. Shumbula, Makwena J. Moloto, Tshinyadzo R. Tshikhudo, Manuel Fernandes, S. Afr. j. sci. **106**, (2010).
[21] M. A. Abdulsattar, Silicon **5**, 229 (2013).
[22] Sidra Farid, Michael A. Stroscio and Mitra Dutta, Super lattices and Microstructures **115**, 204 (2018).
[23] Mudar Ahmed Abdulsattar, Mohammed T. Hussein, Tasneem H. Mahmood, Vacuum **153**, Scopus (2018).
[25] Mohammed T. Hussein, Asmit Ramizy, Bilal K. Ahmed, Vol.15, No.33, PP.54-62, Iraqi Journal of Physics, (2017).